

# Dynamic Response Analysis of A Tall RC Chimney Damaged during 2007 Niigata-ken Chuetsu-Oki Earthquake

**Suhee Kim and Hitoshi Shiohara**

*Def. of Architectural Engineering, School of Engineering, The University of Tokyo, Japan*



## SUMMARY:

Nonlinear dynamic analyses were carried out on a sixty meters high reinforced concrete chimney of an incineration plant in Kashiwazaki, Japan, which was structurally damaged during 2007 Niigata-ken Chuetsu-oki Earthquake, to examine the factors which caused the damage. The effect of the vertical flexural strength distribution of the chimney and the influence of predominant period of the ground motion were investigated. The structural drawings were examined and the failure was found to be occurred at the section where the flexural strength was locally insufficient. In addition to that, the ground motion recorded near the chimney site contained relatively long period component. It is confirmed from the analytical results that a high intensity, long-period ground motion lead the chimney to respond in the high nonlinearity range and the flexural strength discontinuity attracts concentration of inelastic response in the chimney damage mechanism.

*Keywords: Reinforced Concrete chimney, Earthquake Damage, Nonlinear Dynamic response, Flexural strength*

## 1. INSTRUCTION

The 2007 Niigataken Chuets-Oki Earthquake ( $M_w$  6.8) on June 16th caused severe structural damage to a tall reinforced concrete chimney of an incineration plant in Kashiwazaki, with a height of about sixty meters. It was one of the most notable damage to reinforced concrete engineered structures due to the Earthquake. Although this damage did not produce casualties, the industrial facility was out of operation for 4 months until it was restored. The photos of the damage of the chimney are shown in Figure1 [Building Research Institute, 2007].

The chimney was designed to the latest seismic standard and constructed in 1994. In the structural design, the longitudinal reinforcement was determined such that the moment capacity provided exceeded the code's demand, the vertical distribution of which is linearly decreasing over the height. Thus, the actual moment capacity changes showing stepped movement like a set of stair. The structural drawings were examined and the failure was found to be occurred at the level where double layers of longitudinal reinforcing bars were changed to a single layer, which formed a critical flexural strength discontinuity.

The ground motion that was recorded near the chimney site had a relatively long predominant period of 2-2.5 seconds. The long predominant period of the ground motion is considered to be one of the reasons that caused failure of the chimney which has a long natural period.

In this study, a series of nonlinear time history analyses was performed to investigate the effect of discontinuity of vertical strength distribution and the influence of predominant period of the ground motion on the damaged chimney.



**Figure 1.** Damage of the chimney

## 2. THE RECORDED GROUND MOTION NEAR THE CHIMNEY SITE

The 2007 Niigata-ken Chuetsu-Oki Earthquake was a M6.8 quake which hit the northwest Niigata region of Japan. In the city of Kashiwazaki, where the damaged incineration plant is located, seismic intensity of a strong 6 of JMA scale was reported and a time history of strong ground motion was obtained by a K-net station near the chimney. The epicentre of the quake is shown in Figure 2. The locations of the incineration plant and of the observation point of K-net are also shown in Figure 2. The chimney site was at a distance of approximately 18km to the epicentre of the quake and within 3km of the observation point of K-net, NIG018.



**Figure 2.** Location of epicentre, chimney site, and K-net observation point

The maximum ground acceleration and velocity of the three components are shown in Table 1. They were recorded at a K-net station NIG018. The wave forms of the EW and the NS components of the ground acceleration and linear velocity response spectra of a damping factor of 2% are shown in Figure 3. From the response spectra, it is seen that the dominant period of the ground motion is relatively long (from 2 to 2.5 second). Significant contribution to the excitation of the first mode of the chimney is anticipated because the linearly elastic natural period of the first mode for the chimney is approximately 1 second.

**Table 1.** The maximum acceleration and velocity of three components

|               | Measured seismic intensity scale | component | PGA , gal | PGV , kine |
|---------------|----------------------------------|-----------|-----------|------------|
| K-net, NIG018 | 6.4                              | EW        | 514       | 85.9       |
|               |                                  | NS        | 667       | 106.9      |
|               |                                  | UD        | 369       | 25.9       |

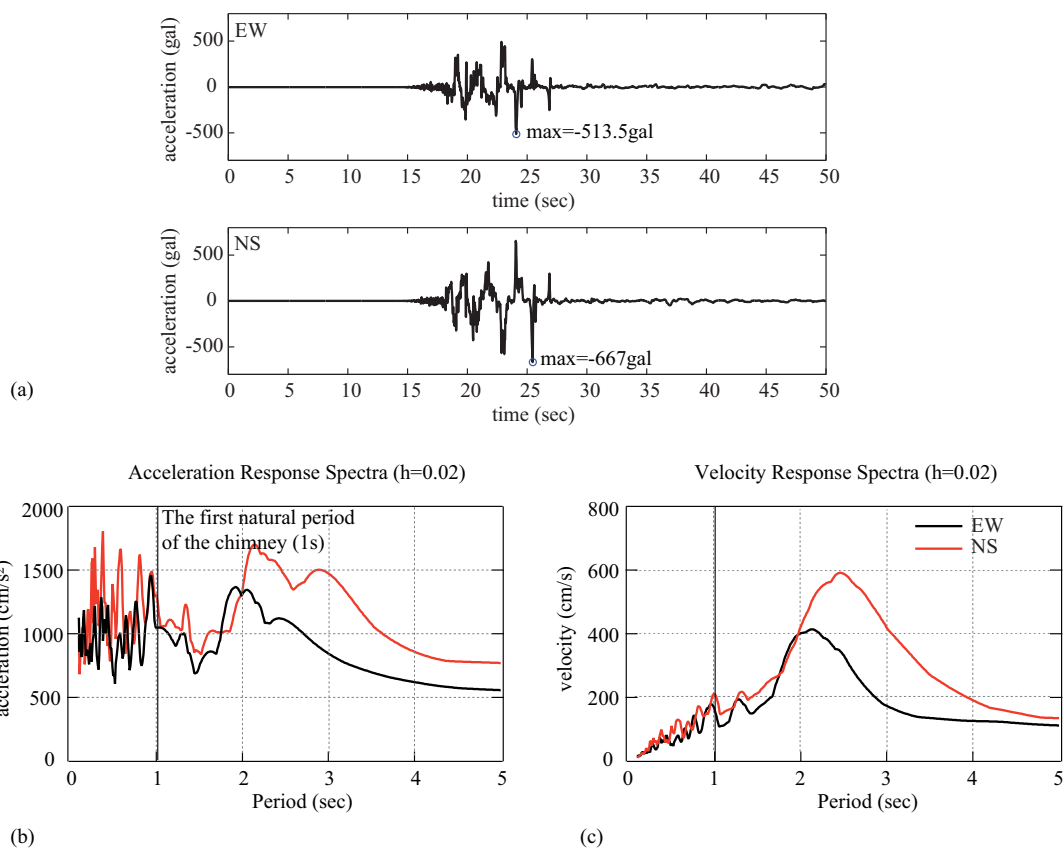


**Figure 3.** (a) Time histories of recorded ground acceleration (b) Acceleration response spectra (damping factor of 0.02) (c) Velocity response spectra (damping factor of 0.02)

### 3. STRUCTURAL CONFIGURATION

#### 3.1. Geometry, dimension and reinforcement

The reinforced concrete (RC) chimney is a cantilever type, and has a box shaped section on the side of which is 4.6 meters long. Two steel air ducts are encased in it. The thickness of the RC box-wall varies from 336mm at base to 180mm at the top. Longitudinal reinforcements are designed to decrease in the height direction. The reinforcements and structural configuration are shown in Figure 4 [Building Research Institute (2007)]. The longitudinal reinforcements are cut-off at six locations; see ② through

⑦ in Figure 4. The chimney damage observed was at a height of approximately 17.5 meters from the ground level, where two layers of longitudinal steel bars (section (a)) were changed to one layer (section (b)). Furthermore, double transverse hoops were changed to a single transverse hoop at the same height. According to construction documents, Table 2 lists the chimney's geometrical properties at each section, including the height  $H$ , average wall-thickness  $t_w$ , and the cross sectional area  $A_c$ , as well as axial load  $N$ , gravity weight  $W_c$ , and designed longitudinal reinforcement ratio  $p_g$ .

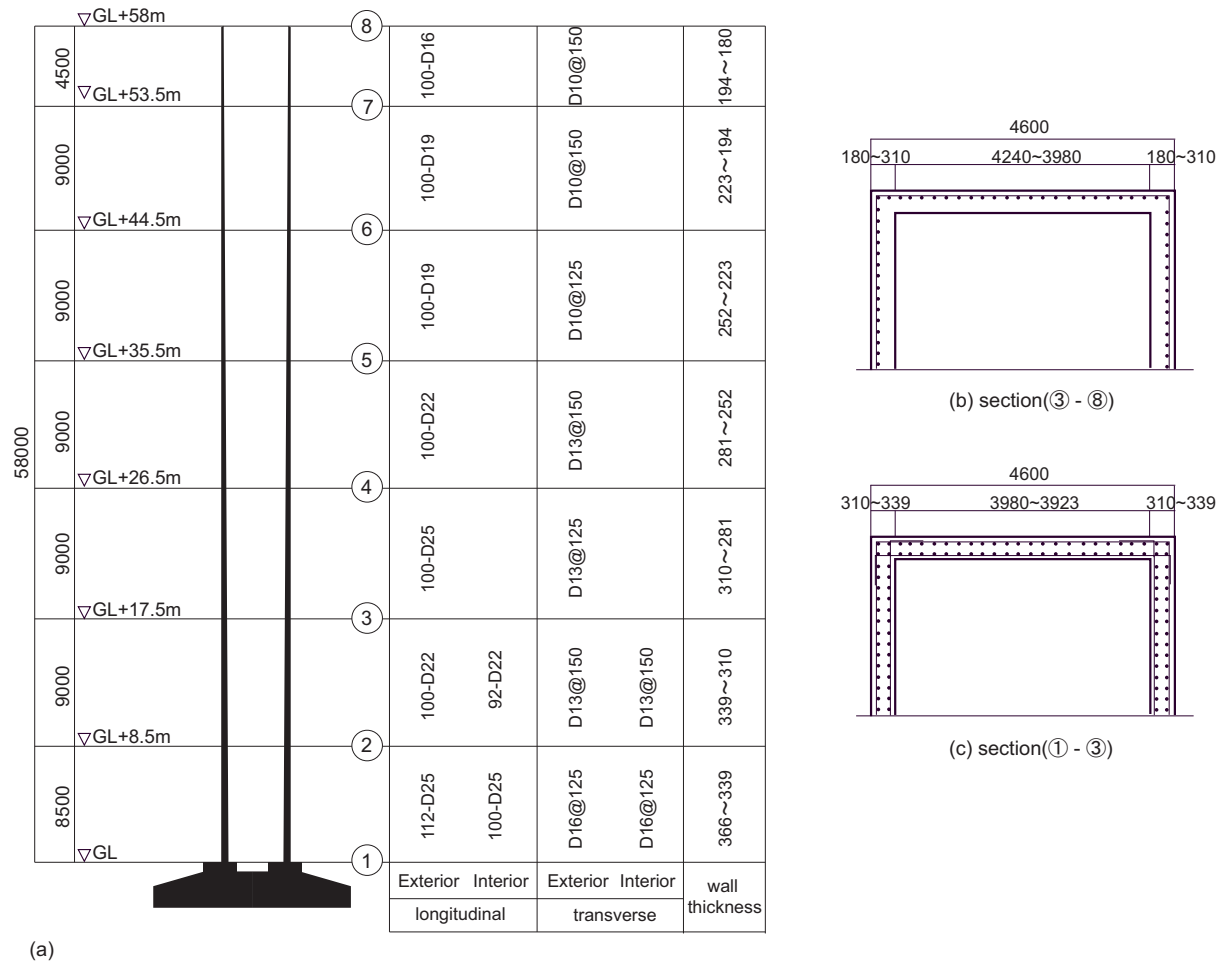


**Figure 4.** (a) Chimney geometry and designed reinforcements (b) Section from level ③ to level ⑧  
(c) Section from level ① to level ③

**Table 2.** Chimney geometry and details

| Level | $t_w$ , m | $A_c$ , m <sup>2</sup> | $W_c$ , kN | $N$ , kN | Designed reinforcement | $P_g$ , % |
|-------|-----------|------------------------|------------|----------|------------------------|-----------|
| ⑦~⑧   | 0.187     | 3.30                   | 356.5      | 356.50   | 100-D16                | 0.65      |
| ⑥~⑦   | 0.208     | 3.66                   | 791.1      | 1147.60  | 100-D16                | 0.56      |
| ⑤~⑥   | 0.237     | 4.14                   | 895.2      | 2042.79  | 100-D19                | 0.71      |
| ④~⑤   | 0.266     | 4.62                   | 997.8      | 3040.60  | 100-D22                | 0.86      |
| ③~④   | 0.295     | 5.09                   | 1099       | 4139.59  | 100-D25                | 1.02      |
| ②~③   | 0.324     | 5.55                   | 1198.7     | 5338.30  | 192-D22                | 1.29      |
| ①~②   | 0.352     | 5.99                   | 1221.8     | 6560.06  | 212-D25                | 1.74      |

### 3.2. Reinforcing detail in the vicinity of the damaged zone

The actual reinforcing detail near the height of 17.5 meters above ground level is shown in Figure 5. It is seen that the locations of lap splice was staggered at this zone. Half of the exterior vertical bars (exterior (A)) were lap spliced at the height of 16 meter while the other half of bars (exterior (B)) were

lap spliced at the height of 17.8 meter. The interior layer of vertical bars was cut-off at the height of around 17.5 meters and no interior vertical bars existed in the upper part. The amounts of vertical reinforcement expected to resist the bending moments at around 17.5 meters are listed in Table 3. The reinforcement ratio at the height of 17.9 meter is lower than those at the other heights above and below. Due to the insufficient development length of the upper 50-D25 steel bars at the region, shown by a square in B layer, calculation assumes that the 50-D25 exterior steel bars in A layer and 50-D22 exterior steel bars in B layer are able to resist the bending moment from 17.5 meters height to 17.9 meters height.

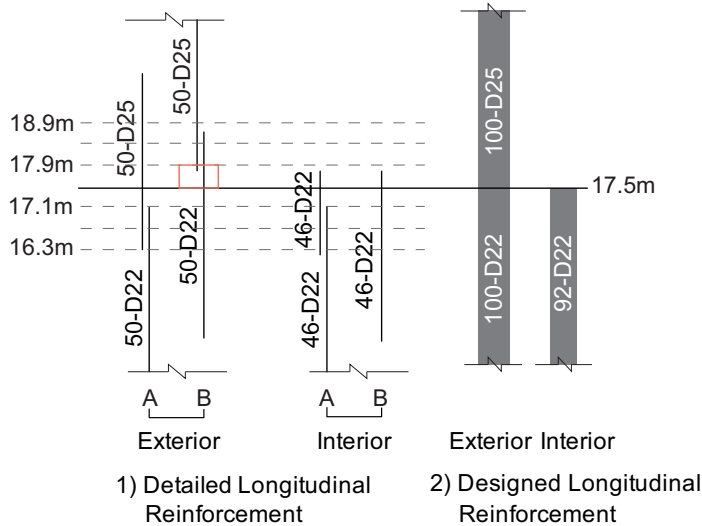


**Table 3.** Reinforcements at around 17.5m

| Height, m | Longitudinal bars |          | $P_g, \%$ |
|-----------|-------------------|----------|-----------|
|           | Exterior          | Interior |           |
| 18.9      | 100-D25           |          | 0.965     |
| 18.4      | 75-D25,<br>25-D22 |          | 0.904     |
| 17.9      | 50-D25<br>50-D22  |          | 0.843     |
| 17.5      | 50-D25<br>50-D22  | 46-D22   | 1.175     |
| 17.1      | 50-D25<br>50-D22  | 92-D22   | 1.500     |
| 16.7      | 100-D22           | 92-D22   | 1.450     |

**Figure 5.** Reinforcing detail at around 17.5meters height

### 3.3. Flexural Strength Comparison

The expected flexural strength of horizontal sections is calculated using the reinforcing detail and is compared with the code demand in Figure 6. The expected flexural strength is calculated at both 0 degree and 45 degree direction of the section. The definition of the flexural strength here is the moment at the first yielding of longitudinal reinforcement in the section. The calculations assumed that the specified concrete compressive is 21MPa and the yield points of reinforcing steel are 295MPa for D16 bar, 345MPa for D19, 22 and 25 bars respectively.

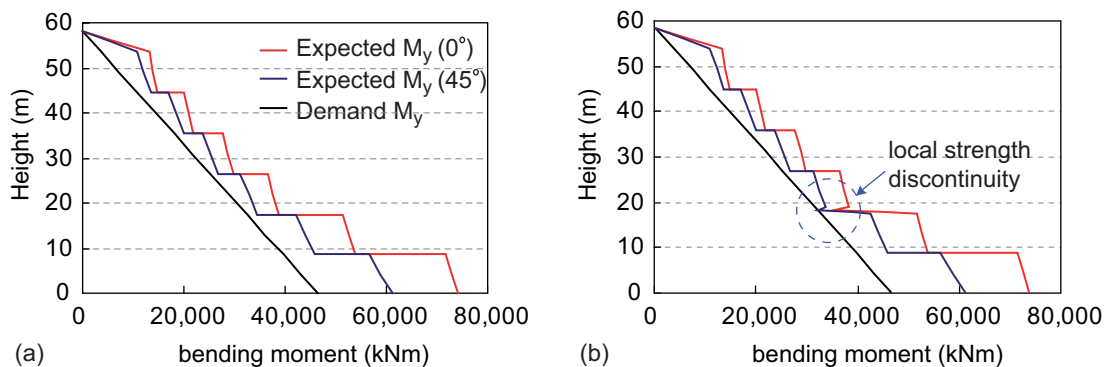


**Figure 6.** (a) Designed flexural strength (b) Flexural strength with sectional deficiency locally at the mid-height.

Two different vertical profiles of flexural strength are shown in Figure 6. One of them is with designed strength profile which considers the six cut-off locations for longitudinal reinforcement (a). The other profile is identical except that the strength of the section is reduced to 90% at the location where the

severe damage was observed (b). This flexural strength is calculated by the reinforcement amount shown in Table 3. Although the flexural strength is still higher than the code demand, the section strength at the 17.5meter height is smaller in comparison with the heights above and below, forming a significant local discontinuity in the strength.

#### 4. ANALYTICAL MODEL

In the analyses, the chimney is modelled as 112 lumped mass elements along the height with connected nonlinear rotational springs to precisely represent the degradation of the stiffness and the strength distribution of the RC cross sections (Figure 7(a)). The elements between mass and nonlinear springs are assumed to be rigid. Tri-linear moment-rotation relationship for the flexural springs determined from sectional analysis and the hysteretic response in the springs is represented by the Takeda hysteretic rule [Toshikazu Takeda et al., 1970]. Table 4 shows the creak moment ( $M_c$ ), yielding moment ( $M_y$ ), and ultimate moment ( $M_u$ ) with according curvature ( $1/\rho_c$ ,  $1/\rho_y$ ,  $1/\rho_u$ ) of each section that used in the analytical model where,  $\alpha$  and  $\beta$  are the post-creak and the post-yield stiffness reduction factors. Figure 8 depicts the moment-curvature relationships. It is also assumed that shear stiffness of the wall is in elastic and the base condition of the chimney is fixed in the analyses. The P-delta effect is considered by taking into account the geometric non-linearity of structures. The nonlinear dynamic response analyses are carried out by the *Newmark- $\beta$*  integration method and Rayleigh viscous damping of 2% proportional to instantaneous stiffness matrix is adopted.

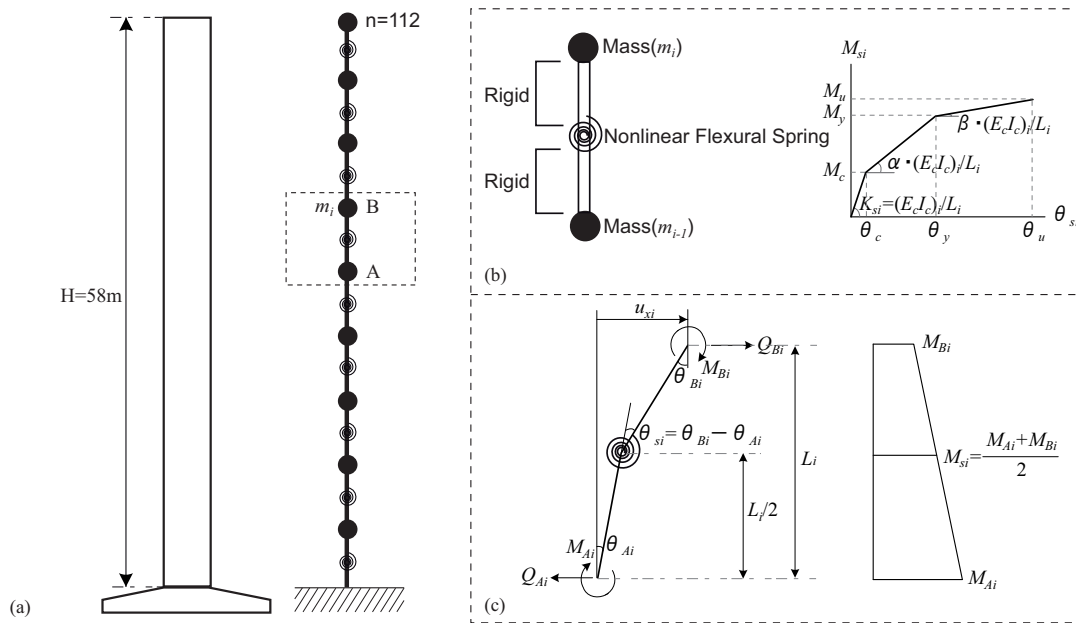


**Figure 7.** (a) Analytical model of the chimney (b) Element model  
(c) Force-deformation relation of an element

**Table 4.** Moment and curvature of the sections

| Height, m | $M_c$ , kNm | $M_y$ , kNm | $M_u$ , kNm | $1/\rho_c$ , rad/m | $1/\rho_y$ , rad/m | $1/\rho_u$ , rad/m | $\alpha$ | $\beta$ |
|-----------|-------------|-------------|-------------|--------------------|--------------------|--------------------|----------|---------|
| 53.5~58   | 11333       | 15279       | 18204       | 5.14E-05           | 4.30E-04           | 4.00E-02           | 0.0150   | 0.0002  |
| 44.5~53.5 | 14747       | 16402       | 20104       | 5.29E-05           | 4.45E-04           | 3.79E-02           | 0.0210   | 0.0005  |
| 35.5~44.5 | 17765       | 20885       | 25613       | 5.70E-05           | 4.60E-04           | 2.90E-02           | 0.0351   | 0.0007  |
| 26.5~35.5 | 20878       | 28700       | 35340       | 6.09E-05           | 4.80E-04           | 2.31E-02           | 0.0647   | 0.0010  |
| 17.5~26.5 | 23983       | 37637       | 46631       | 6.43E-05           | 4.90E-04           | 1.89E-02           | 0.0921   | 0.0015  |
| 8.5~17.5  | 27461       | 52658       | 65957       | 6.84E-05           | 5.20E-04           | 1.32E-02           | 0.1392   | 0.0026  |
| 0~8.5     | 31302       | 72851       | 92424       | 7.31E-05           | 5.50E-04           | 1.05E-02           | 0.2040   | 0.0046  |

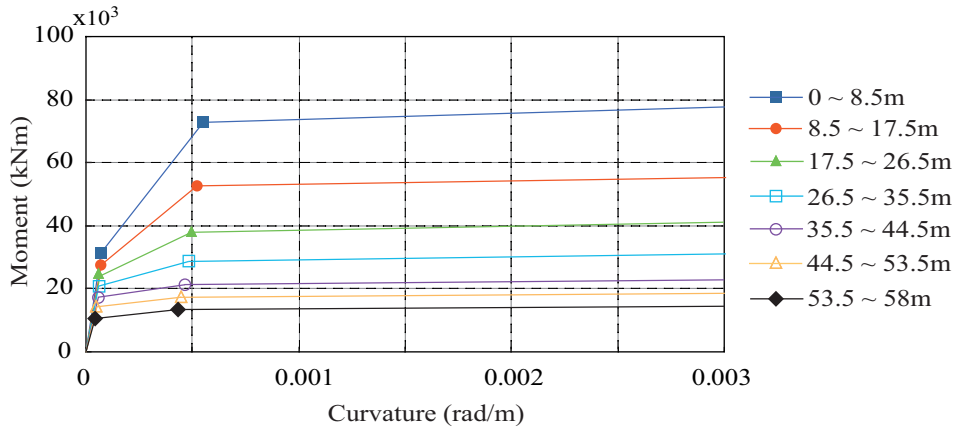


**Figure 8.** Moment versus curvature curve of sections

## 5. INPUT GORUND MOTIONS

Storing ground motions with different predominant periods are used, including Kashiwazaki 2007 motion. The Kobe 1995 motion was recorded in the  $M_w$  6.8 1995 Great Hanshin earthquake and Ojiya 2004 motion was recorded in the  $M_w$  6.8 2004 Chūetsu earthquake of Japan. The 2% damped velocity response spectra of the ground motions are depicted in Figure 9. These two records have a large spectra velocity less than  $T=1.0s$ , which is the first natural period of the damaged chimney.

**Table 5.** List of the ground motions

| Ground motion    | Earthquake  | Observation point | PGA , gal | PGV , kine |
|------------------|---|-------------------|-----------|------------|
| Kobe 1995        | 1995 Great Hanshin Earthquake ( $M_w$ 6.8)            | JMA Kobe (NS)     | 820.56    | 90.82      |
| Ojiya 2004       | 2004 Niigata-ken Chuetsu Earthquake ( $M_w$ 6.8)      | K-net,NIG019 (EW) | 1307.90   | 128.00     |
| Kashiwazaki 2007 | 2007 Niigata-ken Chuetsu -Oki Earthquake ( $M_w$ 6.8) | K-net,NIG01 8(NS) | 667.04    | 106.90     |

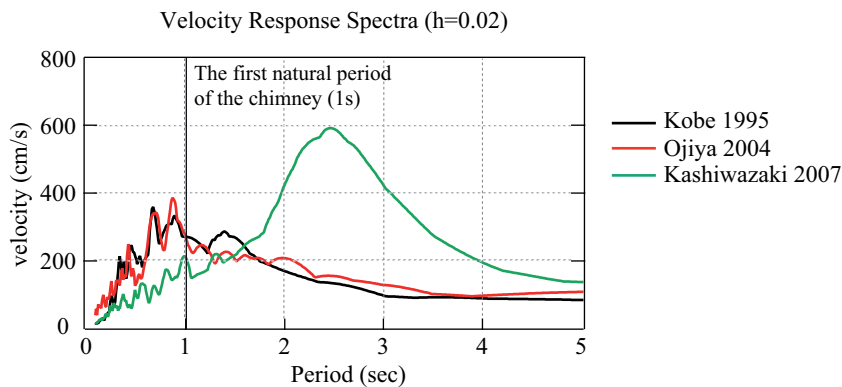


**Figure 9.** Velocity response spectra of the input ground motions (with damping factor of 0.02)

## 6. ANALYTICAL RESULTS

Figure 10 plots the bending moment envelopes obtained from the nonlinear time history analyses for the three ground motions, compared with the capacity. In the analyses, vertical flexural strength capacity that is calculated from the 0 degree direction of the cross-section is used.

It is seen in Figure 10 that the bending moments obtained from the analyses reach or exceed the

capacity in the region of the wall that have flexural discontinuities. The bending moment for the Kashiwazaki 2007 motion shows high demand in the large portion of the wall below mid-height, exceeding the capacity not only at the base but also at around 10 meters and 20 meters height. In contrast, the bending moments obtained for Kobe 1995 and Ojiya 2004 reach the capacity in the upper part of the wall. Considering the predominant periods of the ground motions, the second or higher mode effect is the main reason for the different moment envelope shape. It is observed that the bending moment obtained for all ground motions exceed the flexural strength in the vicinity of the level that has significant strength discontinuity locally.

Figure 11 shows the curvature ductility demands for the three ground motions. Each plot in Figure 10 compares the obtained results when two different vertical strength distributions are used. One of them is when the chimney has expected designed strength (Case1) and the other is when there is critical local strength deficiency in the mid-height (Case2).

For Kashiwazaki 2007 motion, section yielding occurred in every longitudinal reinforcement termination zone below the mid-height in both case 1 and case 2. It is observed that the curvature ductility demand for Kashiwazaki 2007 is much higher than that obtained for the other ground motions. For Kobe 1995 motion, the highest curvature ductility is observed at around 27 meters height of the chimney in Case1 and plasticity at the upper part of the wall is also observed for Ojiya 2004 motion, which is a result of the higher mode effect.

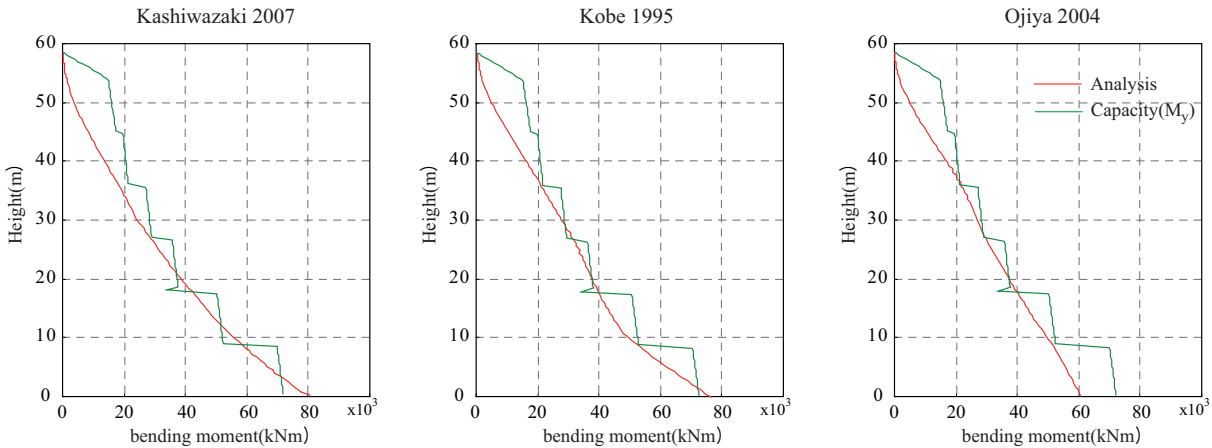


Figure 10. bending moment envelopes obtained from the time history analysis.

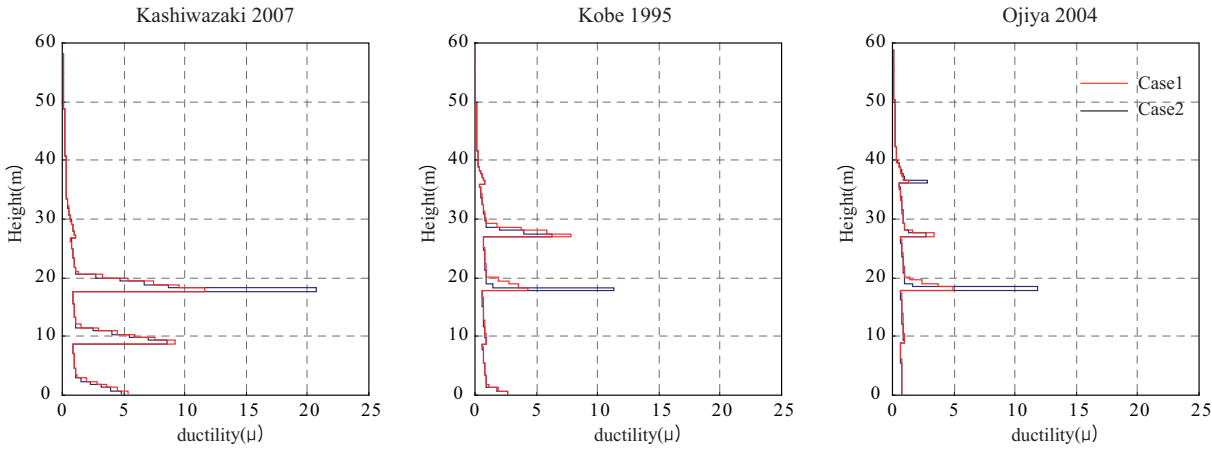


Figure 11. Curvature ductility envelopes obtained from the time history analysis.

It is observed that the yielding occurred at the height of 17.5 meters where the two layers of longitudinal steel bars were changed to one layer for all three ground motions even in case1 (without local strength deficiency). The main difference between the results obtained by the two chimney strength profiles is that the one with degraded section strength yielded a much higher plasticity in the critical section, reaching over twice the degree obtained by the model without section strength degradation.

This analytical result indicates that the 17.5 meters height might be the most critical section in this chimney forming flexural strength discontinuity. This attracted concentration of inelastic response when this chimney was attacked by high intensity, long-period ground motion which led the chimney to respond in high nonlinearity range.

## 7. CONCLUSIONS

A series of nonlinear time history analyses is carried out to investigate the seismic response of the failed chimney. This study includes the influence of predominant periods of the recorded ground motion and the effect of discontinuity of vertical flexural strength distribution of the chimney. Two different vertical strength profiles are considered. One of the models has expected designed strength distribution and the other is identical except strength degradation at the level where the chimney collapsed, which is reduced to 90%. The bending moment envelopes and curvature ductility demands obtained for three ground motions that have different predominant periods are compared. For this study the following results are listed:

- (1) The model with extensive discontinuity in section strength yielded a much higher plasticity in the critical section, reaching over twice the degree obtained by the model without section strength degradation.
- (2) For Kashiwazaki motion, which actually caused failure of the chimney with predominant period of 2 to 2.25 seconds, the bending moment envelopes obtained reached or exceed the code designated flexural strength in most of the sections below the mid-height.

It is concluded that a high intensity, long-period ground motion led the chimney to respond in the high nonlinearity range. Furthermore, the critical flexural strength discontinuity in the mid-height attracts concentration of the inelastic response in the chimney damage mechanism.

## ACKNOWLEDGEMENT

The authors wish to thank the National Research Institute for Earth Science and Disaster Prevention and Japan Meteorological Agency for providing the strong ground motion records.

## REFERENCES

- Architectural Institute of Japan (2007). Structural Design Recommendation for Chimneys.
- Architectural Institute of Japan (2010). AIJ Standard for Structural Calculation of Reinforced Concrete Structures.
- Building Research Institute (2007). Damage of Chimney-like Towers (Reinforced concrete building).
- Toshikazu Takeda, Mete A. Sozen, N. Norby Nieslsen (1970). Reinforced concrete response to simulated earthquakes. *Journal of structural division* **96:12**, 2557-2573.
- Youngsun Kim, Kabeyasawa Toshimi, Kabeyasawa Toshkazu, Kabeyasawa Toshnori (2008). Collapse analysis on a reinforced concrete stack failed during Niigata-ken Chuetsu-oki Earthquake. *Proceedings of the Japan Concrete Institute* **30:3**, 1303-1308